Bulk electroconvective instability at high Péclet numbers

Brian D. Storey
Franklin W. Olin College of Engineering, Needham, Massachusetts 02492, USA

Boris Zaltzman and Isaak Rubinstein
DSEEP, Blaustein Institutes for Desert Research, Ben-Gurion University of the Negev, Sede Boqer Campus, 84990 Israel

(Received 2 May 2007; published 8 October 2007)

Bulk electroconvection pertains to flow induced by the action of a mean electric field upon the residual space charge in the macroscopic regions of a locally quasielectroneutral strong electrolyte. For a long time, controversy has existed in the literature as to whether quiescent electric conduction from such an electrolyte into a uniform charge-selective solid, such as a metal electrode or ion exchange membrane, is stable with respect to bulk electroconvection. While it was recently claimed that bulk electroconvective instability could not occur, this claim pertained to an aqueous, low-molecular-weight electrolyte characterized by an order-unity electroconvection Péclet number. In this paper, we show that the bulk electroconvection model transforms into the leaky dielectric model in the limit of infinitely large Péclet number. For the leaky dielectric model, conduction of the above-mentioned type is unstable, and so it is in the bulk electroconvection model for sufficiently large Péclet numbers. Such instability is sensitive to the ratio of the diffusivity of the cations to the anions. For infinite Péclet number, the case with equal ionic diffusivities is a bifurcation point separating stable and unstable regimes at the low-current limit. Further, for a cation-selective solid, when the Péclet number is finite and the anions are much more diffusive than the cations, an unreported bulk electroconvective instability is possible at low current. At higher currents and large Péclet numbers, we found that the system is unstable for all cation-to-anion diffusivity ratios, but passes from a monotonic instability to an oscillatory one as this ratio passes through unity.

DOI: 10.1103/PhysRevE.76.041501 PACS number(s): 82.45.Gj, 47.20.Ma, 82.39.Wj

I. INTRODUCTION

Flow of electrolyte induced by the action of electric forces on the fluid (electroconvection) on a length scale ranging from nanometers to tens and hundreds of micrometers is an important mechanism in electrochemical transport and microfluidics [1–18]. One of the most fundamental processes in these systems is the one-dimensional steady-state electric conduction from a binary electrolyte solution into a charge-(e.g., for definiteness, positive-charge-)selective solid, such as an electrode (cathode) or ion exchange membrane (cation exchange membrane). The stability of quiescent conduction with respect to a possible onset of electroconvection has been a long studied problem [19–36]. In particular, instability of this configuration has been invoked as a likely source of overlimiting conductance [1,2]. Two modes of electroconvection may be distinguished. The first is bulk electroconvection, which is the flow of an electrolyte due to body forces exerted by an electric field acting upon the residual space charge of a locally quasielectroneutral ionic solution. The second mode is electro-osmosis, in particular, nonequilibrium extended charge electro-osmosis, which is a surface-driven flow originating in the extended space charge region that develops when an electrochemical cell is at the limiting current [3,27–32,36]. This work is concerned only with bulk electroconvection since convection due to extended charge electro-osmotic slip has been thoroughly addressed in recent work [36].

Despite extensive study, whether or not conduction of the aforementioned type is stable to bulk electroconvection has remained unclear [19–25,28,29,33,35]. While it was recently claimed that the bulk electroconvective instability could not occur, this claim pertained to an aqueous, low-molecular-weight electrolyte with order-unity electroconvection Péclet number [29,33,35]. However, when the Péclet number tends to infinity and when the ionic diffusivities are equal, the bulk electroconvection model transforms into the leaky dielectric model [37–40] applied by Hoburg and Melcher to study stability of doped liquid dielectrics [37–39]. In this and related models of liquids with nonuniform electric conductance, the conduction state of the above-mentioned type is unstable [14–16,28,37–39]. Natural questions arise. How do the two models relate to each other, and, in particular, what are the stability characteristics of conduction under bulk electroconvection at large Péclet numbers? The present paper is meant to answer these questions. In addition to its theoretical value, this answer may bear some practical relevance for high-molecular-weight electrolytes.

This paper will show that the existence of bulk electroconvection is sensitive to the ratio of the diffusivity of the cations to the anions. Many previous works on this topic address only the case where the ionic diffusivities are equal. We will show that, when the current is low and the Péclet number is infinite, the situation where the ionic diffusivities are equal is a bifurcation point separating stable and unstable regimes. Further, when the Péclet number is finite, there is still a dramatic difference in the convection when the anions are more diffusive than the cations compared to the opposite case. We will show that when the anions are much more diffusive than the cations an unreported (to the best of our knowledge) bulk electroconvective instability is possible at low current.

We begin Sec. II with the outline of the bulk electroconvection model, yielding the Hoburg-Melcher model and its

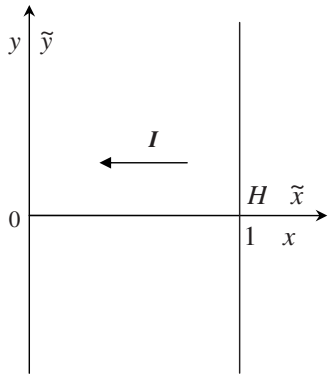

FIG. 1. Sketch of the problem's geometry.

particular generalization termed the modified Hoburg-Melcher model as the infinite-Péclet-number limit (Sec. III). This is followed by formulation of the linear stability problems in all three models (Sec. IV), analyzed analytically in the low-current limit (Sec. V), and numerically for finite currents (Sec. VI).

II. BULK ELECTROCONVECTION IN CONCENTRATION POLARIZATION

Let us consider an infinite planar horizontal layer of thickness H of a univalent electrolyte bounded by two ideally positive charge-selective solid walls, such as cation exchange membranes or metal electrodes, with a constant dc electric current passed upward in the direction normal to the walls. As we will see below, current in this direction induces gravitationally stable density stratification through either electrolyte concentration changes or Joule heating. Moreover, to focus on electroconvection alone, let us assume the layer thickness to be macroscopic but still sufficiently small for any gravity effects to be disregarded altogether here (see Fig. 1 for an illustration of the geometry).

The dimensionless equations for convective electrodiffusion of ions in the layer, together with the Stokes equations and the incompressibility condition, read (we limit ourselves to the planar case for which the linear stability results for our system are identical with those in the three-dimensional case)

$$c_t^+ + (\mathbf{v}\cdot\boldsymbol{\nabla})c^+ = \frac{1}{\mathrm{Pe}}\frac{D+1}{2}\boldsymbol{\nabla}\cdot(\boldsymbol{\nabla}c^+ + c^+\boldsymbol{\nabla}\varphi), \tag{1}$$

$$c_t^- + (\mathbf{v}\cdot\boldsymbol{\nabla})c^- = \frac{1}{\mathrm{Pe}}\frac{D+1}{2D}\boldsymbol{\nabla}\cdot(\boldsymbol{\nabla}c^- - c^-\boldsymbol{\nabla}\varphi), \tag{2}$$

$$\varepsilon^2\Delta\varphi = c^- - c^+, \tag{3}$$

$$\mathrm{Re}\mathbf{v}_t = -\boldsymbol{\nabla}p + \Delta\varphi\boldsymbol{\nabla}\varphi + \boldsymbol{\Delta}\mathbf{v}, \tag{4}$$

$$\boldsymbol{\nabla}\cdot\mathbf{v} = 0 \quad \{0 < x < 1, \quad -\infty < y < \infty\}. \tag{5}$$

The Nernst-Planck equations (1) and (2) describe convective electrodiffusion of cations and anions, respectively. Equation (3) is the Poisson equation for the electric potential, where $c^+ - c^-$ in the right-hand side is the space charge due to a local imbalance of ionic concentrations. The Stokes equation (4) is obtained from the full momentum equation by omitting the nonlinear inertia terms that do not affect the linear stability of the quiescent state studied in this paper. Finally, (5) is the continuity equation for an incompressible solution. The spatial variables in (1)–(5) have been nondimensionalized with the layer thickness H, whereas

$$t = \frac{v_0\tilde{t}}{H}, \quad c^+ = \frac{\tilde{c}^+}{c^0}, \quad c^- = \frac{\tilde{c}^-}{c^0}, \quad \varphi = \frac{F\tilde{\varphi}}{RT} \tag{6}$$

are the dimensionless time, concentrations of cations and anions, and the electric potential. Above, c_0 is the average anion concentration in the layer, F is the Faraday constant, R is the universal gas constant, T is the absolute temperature, and the "salt" diffusivity D_0 is defined as

$$D_0 = \frac{2D_+D_-}{D_+ + D_-}, \tag{7}$$

where D_+ and D_- are the cationic and anionic diffusivities. Furthermore, $\mathbf{v}$ and p in (4) and (5) are the dimensionless velocity vector and pressure, defined as

$$\mathbf{v} = \frac{\tilde{\mathbf{v}}}{v_0} = v_x\mathbf{i} + v_y\mathbf{j}, \quad p = \frac{\tilde{p}}{p_0}, \tag{8}$$

with the typical velocity v_0 and pressure p_0 determined from the force balance in the dimensional version of the momentum equation (4) as

$$v_0 = \frac{d(RT/F)^2}{4\pi\eta H}, \quad p_0 = \frac{\eta v_0}{H}, \tag{9}$$

where d is the dielectric constant of the solution and η is the dynamic viscosity of the fluid. There are four dimensionless parameters in the system (1)–(5) which are as follows.

(1) The dimensionless Debye length ε is defined as

$$\varepsilon = \frac{(dRT)^{1/2}}{2F(\pi c_0)^{1/2}}. \tag{10}$$

ε^2 lies in the range $2\times10^{-13} < \varepsilon^2 < 2\times10^{-5}$ for a realistic macroscopic system with $10^{-4} < H\ (\mathrm{cm}) < 10^{-1}$, $10^{-4} < c_0\ (\mathrm{mol}) < 1$.

(2) The Péclet number Pe is defined as

$$\mathrm{Pe} = \left(\frac{v_0H}{D_0}\right) = \left(\frac{RT}{F}\right)^2\frac{d}{4\pi\eta D_0}. \tag{11}$$

As indicated previously [20], Pe does not depend on c_0 or H. For a typical aqueous, low-molecular-weight electrolyte, Pe is of order unity (more precisely, $\mathrm{Pe}\simeq0.5$).

(3) The relative cationic diffusivity D is defined as

$$D = \frac{D_+}{D_-}. \tag{12}$$

(4) The Reynolds number Re is defined as

$$\mathrm{Re} = \frac{v_0 H}{\nu} = \mathrm{Pe}\frac{D_0}{\nu} = \frac{\mathrm{Pe}}{\mathrm{Sc}}, \tag{13}$$

where ν is the kinematic viscosity of the fluid and Sc is the Schmidt number, typically of the order 10^3 for an aqueous ionic solution.

The extreme smallness of ε^2 motivates the commonly employed approximation of local "stoichiometric" electroneutrality, which amounts to setting $\varepsilon=0$ in (3), yielding

$$c^+ = c^- \overset{\text{def}}{=} c, \tag{14}$$

everywhere in the bulk of electrolyte, except for the boundary (electric double) layers of thickness ε. Note that, although the space charge is very small (of order ε^2) in the Poisson equation (3), it is sufficient to generate an electroconvective flow with Péclet number of order unity through the force term in the Stokes equation (4).

The dimensionless equations for convective electrodiffusion in the local electroneutrality approximation are

$$c_t + (\mathbf{v}\cdot\boldsymbol{\nabla})c = \frac{1}{\mathrm{Pe}}\frac{D+1}{2}\boldsymbol{\nabla}\cdot(\boldsymbol{\nabla}c + c\,\boldsymbol{\nabla}\varphi), \tag{15}$$

$$c_t + (\mathbf{v}\cdot\boldsymbol{\nabla})c = \frac{1}{\mathrm{Pe}}\frac{D+1}{2D}\boldsymbol{\nabla}\cdot(\boldsymbol{\nabla}c - c\,\boldsymbol{\nabla}\varphi). \tag{16}$$

By adding (15) and (16) multiplied by D, we arrive at

$$c_t + (\mathbf{v}\cdot\boldsymbol{\nabla})c = \frac{1}{\mathrm{Pe}}\Delta c. \tag{17}$$

Furthermore, by subtracting (15) from (16), we obtain

$$\frac{D-1}{D+1}\Delta c + \boldsymbol{\nabla}\cdot(c\,\boldsymbol{\nabla}\varphi) = 0. \tag{18}$$

The equations (17) and (18) together with the Stokes equation

$$-\boldsymbol{\nabla}p + \Delta\varphi\,\boldsymbol{\nabla}\varphi + \Delta\mathbf{v} = \mathrm{Re}\,\mathbf{v}_t \tag{19}$$

and continuity equation

$$\boldsymbol{\nabla}\cdot\mathbf{v} = 0 \tag{20}$$

form the final set describing macroscopic bulk electroconvection in the local stoichiometric electroneutrality approximation.

The simplest version of the galvanostatic boundary conditions reads

$$v_x|_{x=0,1} = v_y|_{x=0,1} = 0, \tag{21}$$

$$\left(\frac{\partial c}{\partial x} + c\frac{\partial\varphi}{\partial x}\right)\Bigg|_{x=0,1} = I = \mathrm{const}, \tag{22}$$

$$\left(\frac{\partial c}{\partial x} - c\frac{\partial\varphi}{\partial x}\right)\Bigg|_{x=0,1} = 0, \tag{23}$$

$$\int_\Sigma (c-1)\,dx\,dy = 0. \tag{24}$$

Equations (21) are standard no-slip conditions at the solid boundaries. The current conditions (22) specify a constant electric current density I through the membrane (the expression in parentheses stands for the x component of the dimensionless cationic flux). Conditions (23) state the impermeability of these boundaries for anions (the expression in parentheses stands, with a minus sign, for the x component of the dimensionless anionic flux). These boundary conditions are complemented by periodicity conditions in the y direction. The normalization condition (24), in which integration in y is carried over one period, specifies the total amount of anions in the layer (per unit area of membrane). This condition is necessary for uniqueness of concentration with flux conditions (22) and (23). Hereafter, we shall refer to the problem (17)–(24) as the bulk electroconvection (BE) model.

The steady state version of the boundary value problem (17)–(24) possesses a trivial quiescent conduction (concentration polarization) solution:

$$c_0(x) = 1 + \frac{I}{2}\left(x - \frac{1}{2}\right), \quad \varphi_0(x) = \ln\left[1 + \frac{I}{2}\left(x - \frac{1}{2}\right)\right], \tag{25}$$

$$\mathbf{v}_0 \equiv \mathbf{0}, \quad p_0(x) = \frac{1}{2}\varphi_{0x}^2 + \mathrm{const}. \tag{26}$$

Expression (25) yields the current-voltage relation,

$$I = 4\frac{1-e^{-V}}{1+e^{-V}}, \tag{27}$$

where

$$V \overset{\text{def}}{=} \varphi_0(1) - \varphi_0(0) \tag{28}$$

is the voltage across the solution.

From (27), when $V\to\infty$, $I\to I^{\mathrm{lim}}=4$, and, simultaneously, by (25), $c_0(0)\to 0$. This is the key feature of the classical picture of the concentration polarization—saturation of the current density toward the limiting value with increasing voltage, resulting from the vanishing interface electrolyte concentration at the cathode.

III. INFINITE-PÉCLET-NUMBER ASYMPTOTICS AND TRANSITION TO HOBURG-MELCHER ELECTROCONVECTION IN DOPED DIELECTRICS

The model of electroconvection in doped dielectrics introduced by Hoburg and Melcher (HM) (see Refs. [37–40]) is obtained from the BE model (17)–(24) by setting equal diffusivities of co- and counterions in Eq. (18) ($D=1$; see Ref. [33]) and assuming $\mathrm{Pe}\gg 1$ while keeping the leading-order term in Eq. (17), which yields

$$c_t + (\mathbf{v}\cdot\boldsymbol{\nabla})c = 0, \tag{29}$$

TABLE I. Different equations in various models.

BE model	MHM model $D \neq 1$, $\mathrm{Pe} \to \infty$	HM model $D=1$, $\mathrm{Pe} \to \infty$
$c_t + (\mathbf{v}\cdot\nabla)c = \frac{1}{\mathrm{Pe}}\Delta c$	$c_t + (\mathbf{v}\cdot\nabla)c = 0$	
$\frac{D-1}{D+1}\Delta c + \nabla\cdot(c\nabla\varphi) = 0$	$\nabla\cdot(c\nabla\varphi) = 0$	

$$\nabla \cdot (c\,\nabla\,\varphi) = 0, \tag{30}$$

$$-\nabla p + \Delta\varphi\,\nabla\,\varphi + \Delta\mathbf{v} = \mathrm{Re}\,\mathbf{v}_t, \tag{31}$$

$$\nabla \cdot \mathbf{v} = 0. \tag{32}$$

The no-slip conditions (21) at the solid boundaries, and the migration term of the electric current at the solid/liquid interface

$$c\frac{\partial\varphi}{\partial x}\bigg|_{x=0,1} = \frac{I}{2}, \tag{33}$$

together with periodicity conditions in y, complete the HM model.

We consider also the modified Hoburg-Melcher (MHM) formulation, assuming the Péclet number to be large, $\mathrm{Pe} \gg 1$, and $D \neq 1$, which to the leading order yields

$$c_t + (\mathbf{v}\cdot\nabla)c = 0, \tag{34}$$

$$\frac{D-1}{D+1}\Delta c + \nabla\cdot(c\,\nabla\,\varphi) = 0, \tag{35}$$

$$-\nabla p + \Delta\varphi\,\nabla\,\varphi + \mathbf{v} = \mathrm{Re}\,\mathbf{v}_t, \tag{36}$$

$$\nabla \cdot \mathbf{v} = 0, \tag{37}$$

$$v_x|_{x=0,1} = v_y|_{x=0,1} = 0, \tag{38}$$

$$\left(\frac{D-1}{D+1}\frac{\partial c}{\partial x} + c\frac{\partial\varphi}{\partial x}\right)\bigg|_{x=0,1} = \frac{DI}{D+1}. \tag{39}$$

We note that all three models are identical except for the transport and current continuity equations. To ease the comparison we list the differing equations in Table I.

IV. LINEAR STABILITY OF QUIESCENT CONCENTRATION POLARIZATION IN THREE MODELS

In this section we formulate the linear stability problems for concentration polarization solution (17)–(24) in the HM, MHM, and BE models. For this, we assume an infinitesimal flow $\mathbf{v}'$ which creates small two-dimensional fluctuations c', p', φ' in the concentration, pressure, and electrostatic potential. Let us consider a perturbation of the conduction solution (25) and (26) of the form

$$\begin{pmatrix} c_0(x) \\ \varphi_0(x) \\ \mathbf{v}_0 \equiv 0 \\ p_0(x) \end{pmatrix} + \begin{pmatrix} \xi(x)\exp(iky) \\ \Phi(x)\exp(iky) \\ \mathbf{V}(x)\exp(iky) \\ P(x)\exp(iky) \end{pmatrix} e^{st} \tag{40}$$

where $\mathbf{V}(x) = u(x)\mathbf{i} + w(x)\mathbf{j}$.

Substitution of Eq. (40) into the BE problem (17)–(24), followed by linearization, yields a spectral problem for (ξ, Φ, u) and s with the equations

$$u = \frac{2}{I}\left(\frac{1}{\mathrm{Pe}}\mathbf{L} - s\right)\xi, \tag{41}$$

$$\mathbf{L}^2[u] - \mathrm{Re}\,s\mathbf{L}[u] = k^2\frac{I}{2 + I(x-1/2)}\mathbf{L}[\Phi] - 2k^2\left(\frac{I}{2 + I(x-1/2)}\right)^3\Phi, \tag{42}$$

$$\frac{D-1}{D+1}\mathbf{L}[\xi] + \frac{I}{2}\frac{d\Phi}{dx} + \left[1 + \frac{I}{2}\left(x - \frac{1}{2}\right)\right]\mathbf{L}[\Phi] + \frac{d}{dx}\left(\frac{I}{2 + I(x-1/2)}\xi\right) = 0, \tag{43}$$

where

$$\mathbf{L} = \frac{d}{dx^2} - k^2. \tag{44}$$

The boundary conditions are

$$\frac{d\xi}{dx}\bigg|_{x=0} = \left(\frac{I/2}{1 - I/4}\xi + (1 - I/4)\frac{d\Phi}{dx}\right)\bigg|_{x=0} = u|_{x=0} = \frac{du}{dx}\bigg|_{x=0} = 0, \quad x = 0 \quad \text{(anode)}, \tag{45}$$

$$\frac{d\xi}{dx}\bigg|_{x=1} = \left(\frac{I/2}{1 + I/4}\xi + (1 + I/4)\frac{d\Phi}{dx}\right)\bigg|_{x=1} = u|_{x=1} = \frac{du}{dx}\bigg|_{x=1} = 0, \quad x = 1 \quad \text{(cathode)}. \tag{46}$$

In the limit of infinitely large Péclet number, the eight-order spectral problem (41)–(46) is reduced to the following sixth-order one representing the MHM model:

$$u = -\frac{2s}{I}\xi, \tag{47}$$

$$\frac{D-1}{D+1}\mathbf{L}[\xi] + \frac{I}{2}\frac{d\Phi}{dx} + \left[1 + \frac{I}{2}\left(x - \frac{1}{2}\right)\right]\mathbf{L}[\Phi] + \frac{d}{dx}\left(\frac{I}{2 + I(x-1/2)}\xi\right) = 0, \tag{48}$$

$$\mathbf{L}^2[u] - s\,\mathrm{Re}\,\mathbf{L}[u] = k^2 \frac{I}{2 + I(x - 1/2)} \mathbf{L}[\Phi] - 2k^2 \left(\frac{I}{2 + I(x - 1/2)} \right)^3 \Phi. \quad (49)$$

Equation (47) together with no slip at the solid/liquid interfaces yields

$$\xi(0) = \xi(1) = 0, \quad (50)$$

and, thus, the boundary conditions read

$$\left. \frac{d\Phi}{dx} \right|_{x=0,1} = u|_{x=0,1} = \left. \frac{du}{dx} \right|_{x=0,1} = 0. \quad (51)$$

The HM formulation corresponds to setting $D=1$ in Eq. (48), which removes the first term of this equation.

V. LINEAR STABILITY ANALYSIS OF THE LOW-CURRENT LIMIT

In this section we analyze the problems (41)–(46) and (47)–(51) in the low-current ($I \ll 1$) limit. We first consider the limit of infinite Péclet number in the Hoburg-Melcher and modified Hoburg-Melcher models. We then analyze the transition to finite Péclet numbers in the bulk electroconvection model.

A. Hoburg-Melcher model, Pe$\to\infty$, $D=1$

Let us start with the original Hoburg-Melcher formulation [Eqs. (47)–(51) with $D=1$]. For $I \to 0$, Eq. (48) yields the following relation between $\mathbf{L}[\Phi]$ and $d\xi/dx$:

$$\mathbf{L}[\Phi] + \alpha \frac{d\xi}{dx} = 0; \quad (52)$$

here $\alpha = I/2$; whereas Eq. (49) yields

$$\mathbf{L}^2[u] - s\,\mathrm{Re}\,\mathbf{L}[u] = k^2 \alpha \mathbf{L}[\Phi]. \quad (53)$$

Substitution of Eq. (52) into Eq. (53) yields a fourth-order equation,

$$S_1 \mathbf{L}^2[u] - S_1^2 \alpha^3\,\mathrm{Re}\,\mathbf{L}[u] - k^2 \frac{du}{dx} = 0, \quad (54)$$

where

$$S_1 = \frac{s}{\alpha^3}. \quad (55)$$

Let us note that the scaling Eq. (55) is particular for this formulation with $D=1$. Keeping leading terms in Eq. (54), we obtain

$$S_1 \mathbf{L}^2[u] - k^2 \frac{du}{dx} = 0, \quad (56)$$

which together with the no-slip conditions

$$\left. \frac{du}{dx} \right|_{x=0,1} = u|_{x=0,1} = 0 \quad (57)$$

forms the linear stability problem for the HM model at low current.

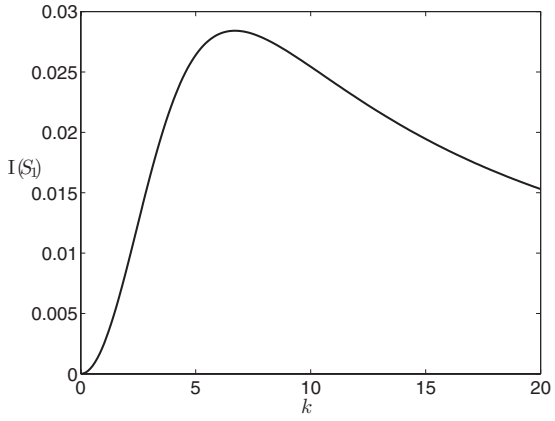

FIG. 2. Imaginary part of the dominant eigenvalue S_1 as a function of wave number as computed from the low-current HM model.

The numerical solution of the problem (56) and (57) yields a purely imaginary spectrum with an accumulation point at the origin. This is the expression of singularity of this limiting formulation. This singularity is based in the spectrum parameter in Eq. (56), which multiplies the highest derivative instead of multiplying in the dominant second power the lower-order derivative in Eq. (54). Correspondingly, this singularity is removed by returning for a finite α from Eq. (56) to Eq. (54). In Fig. 2 we present the dependence of the imaginary part of the eigenvalue with the largest absolute value on the wave number k.

B. Modified Hoburg-Melcher model, Pe$\to\infty$, $D\neq 1$

Turning to the modified Hoburg-Melcher model, that is, Eqs. (47)–(51) with $D \neq 1$, the limiting low-current spectral problem assumes the form

$$u = -\frac{s}{\alpha}\xi, \quad (58)$$

$$\frac{D-1}{D+1}\mathbf{L}[\xi] + \mathbf{L}[\Phi] = 0, \quad (59)$$

$$\mathbf{L}^2[u] - s\,\mathrm{Re}\,\mathbf{L}[u] = k^2 \alpha \mathbf{L}[\Phi]. \quad (60)$$

This case is simpler than the degenerate case $D=1$ because Eq. (59), as opposed to Eq. (52), establishes a relation between $\mathbf{L}[\Phi]$ and $\mathbf{L}[\xi]$. Substitution of this relation into Eq. (60) yields

$$S_2 \mathbf{L}^2[u] - S_2^2 \alpha^2\,\mathrm{Re}\,\mathbf{L}[u] = -k^2 \frac{D-1}{D+1}\mathbf{L}[u], \quad (61)$$

which is a second-order equation for $\mathbf{L}[u]$. Note that

$$S_2 = \frac{s}{\alpha^2} \quad (62)$$

contains the scaling α^2 instead of α^3 in Eq. (62). To leading order in α, Eq. (61) is reduced to

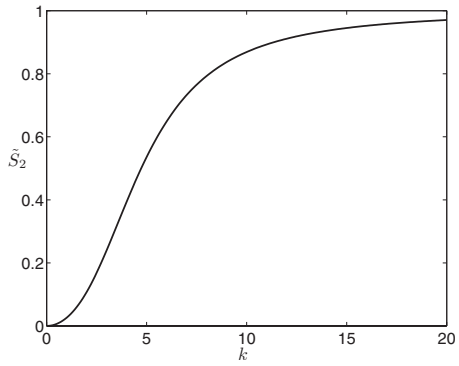

FIG. 3. Dominant eigenvalue S_2 as a function of wave number as computed from the low-current MHM model.

$$S_2\mathbf{L}^2[u] + k^2\frac{D-1}{D+1}\mathbf{L}[u] = 0, \tag{63}$$

which together with the no-slip boundary conditions (57) forms the limiting spectral problem for the MHM model.

Seeking the solution of Eq. (63) in the form

$$u = A\sinh kx + B\cosh kx + C\sinh k\sqrt{1-\frac{1}{\tilde{S}_2}}x + D\cosh k\sqrt{1-\frac{1}{\tilde{S}_2}}x \tag{64}$$

and applying the boundary conditions (57) yields the equation for $\tilde{S}_2$,

$$2\sqrt{1-\frac{1}{\tilde{S}_2}}\left(1-\cosh k\cosh\sqrt{1-\frac{1}{\tilde{S}_2}}k\right) + \left(2-\frac{1}{\tilde{S}_2}\right)\sinh k\sinh\sqrt{1-\frac{1}{\tilde{S}_2}}k = 0, \tag{65}$$

where

$$\tilde{S}_2 = S_2\frac{D+1}{1-D}. \tag{66}$$

Numerical solution of Eq. (65) shows that all $\tilde{S}_2$ are real and positive and accumulate at 0. Once more, this accumulation is regularized (removed) by returning from Eq. (63) to Eq. (61). The eigenvalues to the problem Eqs. (57) and (61) form an unbounded infinite decreasing sequence. The number of eigenvalues lying in the vicinity of 0 increases upon decreasing α, so that in the singular limit, $\alpha=0$, boundedness of the spectrum appears with accumulation at the origin. Taking into account the definition (66) of $\tilde{S}_2$, the sign of S_2 coincides with that of $1-D$. This implies stability for $D>1$ and monotonic instability for $D<1$, separated by marginally stable low-frequency ($S_1=S_2\alpha$) oscillations in the degenerate case ($D=1$) corresponding to the original Hoburg-Melcher model. In Fig. 3 we present the dependence of the maximal modified eigenvalue $\tilde{S}_2$ on k in the singular limit $\alpha=0$.

C. Bulk electroconvection model, $D\neq 1$

We now turn to the BE formulation (41)–(46) and start with a case of nonequal diffusivities $D\neq 1$. The limiting low-current spectral problem analogous to (47)–(51), (57), and (63) assumes the form

$$\mathbf{L}^3[\xi] - s(\mathrm{Pe}+\mathrm{Re})\mathbf{L}^2[\xi] + \mathrm{Pe}\left(\mathrm{Re}\,s^2 + k^2\alpha^2\frac{D-1}{D+1}\right)\mathbf{L}[\xi] = 0, \tag{67}$$

with the following boundary conditions:

$$\left.\frac{d\xi}{dx}\right|_{x=0,1} = \left.\left(\frac{1}{\mathrm{Pe}}\frac{d^2\xi}{dx^2} - \left(\frac{k^2}{\mathrm{Pe}}+s\right)\xi\right)\right|_{x=0,1} = \left.\frac{d^3\xi}{dx^3}\right|_{x=0,1} = 0. \tag{68}$$

Keeping leading-order terms in Eq. (67) and assuming $\mathrm{Re}=O(1)$, we find

$$\mathbf{L}^3[\xi] - S_3\mathbf{L}^2[\xi] + \mathrm{Pe}_1k^2\frac{D-1}{D+1}\mathbf{L}[\xi] = 0, \tag{69}$$

$$\left.\frac{d\xi}{dx}\right|_{x=0,1} = \left.\left(\frac{d^2\xi}{dx^2} - (k^2+S_3)\xi\right)\right|_{x=0,1} = \left.\frac{d^3\xi}{dx^3}\right|_{x=0,1}, \tag{70}$$

where

$$\mathrm{Pe}_1 = \mathrm{Pe}\,\alpha^2, \quad S_3 = s\,\mathrm{Pe} = \frac{s}{\alpha^2}\mathrm{Pe}_1. \tag{71}$$

We seek the solution of Eq. (69) in the form

$$\xi = A\sinh kx + B\cosh kx + C\sinh k\sqrt{1+\lambda_1}x + D\cosh k\sqrt{1+\lambda_1}x + E\sinh k\sqrt{1+\lambda_2}x + F\cosh k\sqrt{1+\lambda_2}x, \tag{72}$$

where

$$\lambda_{1,2} = \frac{1}{2}\sqrt{\frac{S_3}{k^2} \pm \sqrt{\left(\frac{S_3}{k^2}\right)^2 + 4\frac{L}{k^2}}}, \quad L = \mathrm{Pe}_1\frac{D-1}{D+1}. \tag{73}$$

Substituting Eq. (72) into boundary conditions (70) and solving the obtained transcendental equation for S_3 (we do not present this solution here due to its lengthiness and technical character), we find that all S_3 are real. In Fig. 4 we present the dependence of the largest eigenvalue S_3^0 on k for two values of the control parameter L ($L=-100, 100$). Figure 4 shows that the system can become unstable with respect to bulk electroconvection when $D<1$.

Substitution of $S_3=0$ into Eqs. (70), (72), and (73) yields the following equation for the marginal stability curve:

$$\frac{\sqrt{1+\sqrt{1+L/k^2}}}{\sinh k\sqrt{(1+\sqrt{1+L/k^2})/2}} = \pm\frac{\sqrt{\sqrt{1+L/k^2}-1}}{\sin k\sqrt{(\sqrt{1+L/k^2}-1)/2}}. \tag{74}$$

In Fig. 5 we present the dependence of the parameter L on k for marginal stability when $D<1$. When $D<1$ the system is

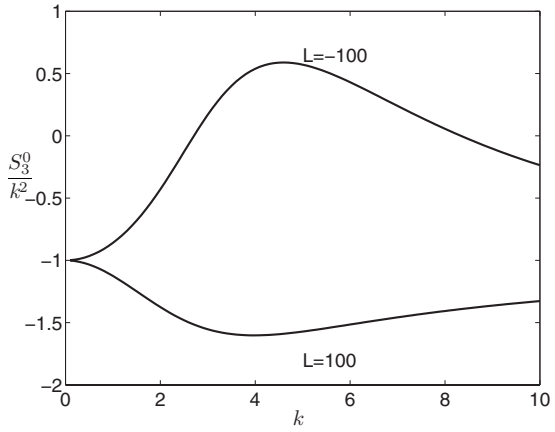

FIG. 4. Wave number dependence of the dominant eigenvalue for the BE formulation at low current, S_3^0. When $L=-100$, the system has a band of wave numbers where the growth rates are positive and the system is unstable, corresponding to $D<1$. When $L=100$, the system is stable, corresponding to $D>1$.

unstable when $-L$ exceeds the threshold value of $L=-68$. A positive value of L yields the stability of low-current ($\alpha \ll 1$) one-dimensional conduction for $D \geqslant 1$ and Pe $\leqslant O(1/\alpha^2)$.

We wish to point out that Eq. (70) obtained in the low-current and infinite-Péclet-number limit, corresponding to constant concentration (conductivity) in the base state and vanishing contribution of diffusion, is reminiscent of the approximate spectral equation in the leaky dielectric model of suspended fluid film stability by Daya *et al.* [41]. This latter model, also employing constant conductivity and negligible charge diffusion assumptions, yields a critical wave number 4.744 compared to 4.74 in Fig. 5, a striking manifestation of similarity between the two models.

D. Bulk electroconvection model, $D=1$

Let us now consider the $D=1$ case in the BE formulation. The low-current spectral problem at $D=1$ assumes the form

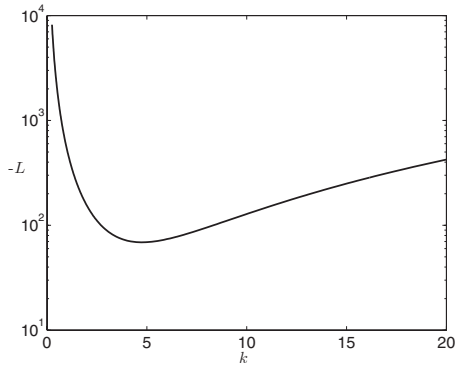

FIG. 5. Marginal stability curve for the BE formulation when $D<1$; the minimum corresponds to critical values $L_c \equiv \text{Pe}\,\alpha^2(D-1)/(D+1)=-68$, $k_c=4.74$.

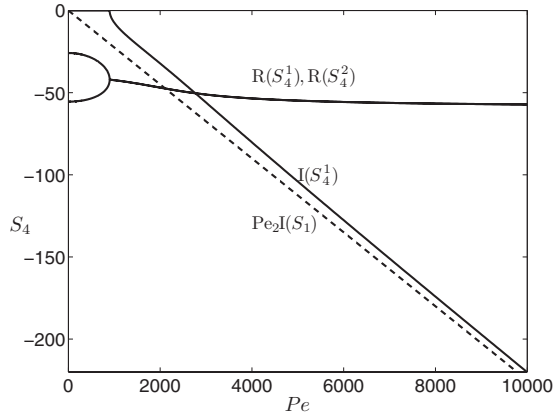

FIG. 6. Real and imaginary parts of the eigenvalues S_4^1 and S_4^2 as a function of Péclet number for $k=4$. The two real eigenvalues merge around $\text{Pe}_2^*=900$ and form a complex conjugate pair. As the Péclet number increases to infinity, the eigenvalues computed from the BE model converge to those computed from the HM model.

$$\mathbf{L}^3[\xi] - s(\text{Pe}+\text{Re})\mathbf{L}^2[\xi] + \text{Pe Re}\, s^2\mathbf{L}[\xi] + \text{Pe}\, k^2\alpha^3\frac{d\xi}{dx} = 0, \tag{75}$$

with the same boundary conditions (68) as in the previous section.

Keeping leading-order terms in Eq. (75) and assuming $\text{Re}=O(1)$ we find

$$\mathbf{L}^3[\xi] - S_4\mathbf{L}^2[\xi] + \text{Pe}_2 k^2\frac{d\xi}{dx} = 0, \tag{76}$$

$$\left.\frac{d\xi}{dx}\right|_{x=0,1} = \left.\left(\frac{d^2\xi}{dx^2} - (k^2+S_4)\xi\right)\right|_{x=0,1} = \left.\frac{d^3\xi}{dx^3}\right|_{x=0,1} = 0, \tag{77}$$

where

$$\text{Pe}_2 = \text{Pe}\,\alpha^3, \quad S_4 = s\,\text{Pe} = \frac{s}{\alpha^3}\text{Pe}_2. \tag{78}$$

Numerical solution of Eqs. (76) and (77) shows that all eigenvalues S_4 have a negative real part and the first eigenvalue S_4^0 is real and negative.

Finally, sending Pe_2 to ∞ in problem (76) and (77) yields the following convergence of all complex eigenvalues S_4 to the respective eigenvalues of the problem (56) and (57), S_1:

$$\frac{S_4}{\text{Pe}_2} \to S_1. \tag{79}$$

In Fig. 6 we present the dependence of the second and third eigenvalues S_4^1 and S_4^2 (the first one S_4^0 is equal to $-k^2$ and does not depend on Pe_2) on Pe_2 for $k=4$. Let us note the merging of the pair of real eigenvalues S_4^1 and S_4^2 followed by their splitting into a complex conjugate pair at the threshold Pe_2^*.

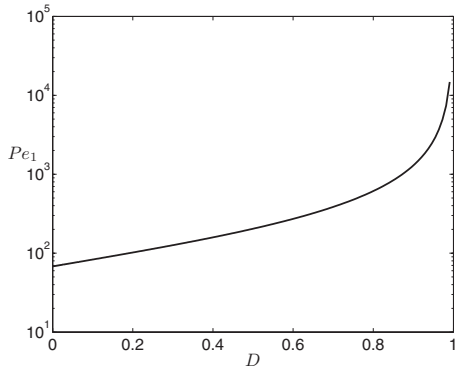

FIG. 7. Critical Péclet number as a function of D at low current. The system is unstable when Pe exceeds this critical value. When $D>1$ the low-current analysis predicts that the system is always stable. Note that the y axis uses $\mathrm{Pe}_1=\mathrm{Pe}\,\alpha^2$ from Eq. (71).

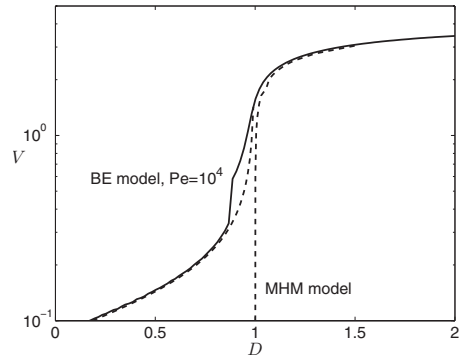

FIG. 8. Critical voltage as a function of D at high Péclet number at $k=4$. The solid curve is computed from the BE formulation; the two dashed curves are computed from the low-current formulation for $D<1$ and the MHM model for $D>1$.

E. Summary of low-current results

At low current, both the MHM and BE models predict that the system is stable when $D>1$. When $D<1$, the MHM model predicts instability. However, when the Péclet number is taken to be finite in the BE model, the system is unstable only when the parameter L exceeds a critical threshold as shown in Fig. 5. The stability results of this section can be summarized by Fig. 7 where we show the critical Péclet number as a function of D. Note that in Fig. 7 the critical parameter is $\mathrm{Pe}_1=\mathrm{Pe}\,\alpha^2$.

From Fig. 7 we can see that the critical Péclet number increases as $D\to 1$. The scaling for Pe_1 shows that the critical Péclet number increases as $\alpha\to 0$, a behavior consistent with the MHM model; at infinite Pe there is always instability. Finally, by applying this low-current analysis outside its region of validity for $\alpha\to 2$, corresponding to the limiting current, we find that that for $D\to 0$ the minimum Péclet number for which instability occurs is approximately $\mathrm{Pe}=17$. As we will see in the next section, this result is modified when proper account is taken of the finite current.

VI. LINEAR STABILITY ANALYSIS AT FINITE CURRENT

In this section we analyze the bulk electroconvection problem at finite current. First, we solve the BE model at large Péclet number such that we can compare that model to results obtained from the limiting MHM model. We then consider how the results with the BE model change as the Péclet number decreases toward more realistic values. All results presented in this section are not amenable to analytical solutions, so in each case we compute the stability numerically. The results presented in this section allow one to determine whether a given system would be subject to bulk electroconvection.

A. Bulk electroconvection model, large Péclet numbers

We first consider the case when the Péclet number is very large and set $\mathrm{Pe}=10^4$ in the BE model. At a fixed k, we can compute the critical voltage as the function of D. The solid curve in Fig. 8 is obtained from a numerical solution of the BE problem for various values of D. The behavior of the BE model when $D<1$ can be understood in terms of the low-current behavior. With the Péclet number taken finite in the BE formulation and $D<1$, we found in the low-current limit that there is a control parameter $L\equiv \mathrm{Pe}\,\alpha^2(D-1)/(D+1)$ which determines the stability. Fixing Pe and knowing the critical value of L, we can readily solve for the critical current (voltage). It is easy to see from the definition of the parameter L that, as $D\to 1$, α must increase sharply to maintain instability. The critical voltage predicted from the low-current results at $\mathrm{Pe}=10^4$ and $k=4$ is shown as the dashed curve in the region $D<1$ of Fig. 8. We see that for $D\ll 1$ the critical voltage is well predicted by the low-current asymptotics. As D increases toward unity, and thus α increases, this approximation is no longer valid and the BE solution departs from its low-current asymptotics. When $D>1$, both the MHM and BE models predict stability at low-current. For $D>1$ and current near the limiting value and exceeding some threshold, the system becomes unstable. The dashed curve in the region $D>1$ is computed from the MHM model at finite current. As seen in Fig. 8, in this region the results for both models conform, whereas around $D=1$ the BE formulation transitions from one limiting behavior to the other.

In the low-current limit of the MHM model, we found that there was monotonic instability when $D<1$ and stability for $D>1$, with stable oscillations at $D=1$. At higher currents and high Péclet number, we find that the system is unstable for all D but passes from a monotonic instability to an oscillatory one as D passes through 1. This is shown in Fig. 9 where we plot the two most dominant eigenvalues as a function of D at high Péclet number ($\mathrm{Pe}=10^4$), near limiting current ($V=4$), and $k=4$. The real part of the eigenvalues are plotted as solid lines and the magnitude of the imaginary part as the dashed line. We observe a merger of the two largest real eigenvalues which split into complex conjugates at $D=1$.

B. Bulk electroconvection model, moderate Péclet numbers

We now compare the stability results for the BE formulation at finite current to those in the low- current limit when

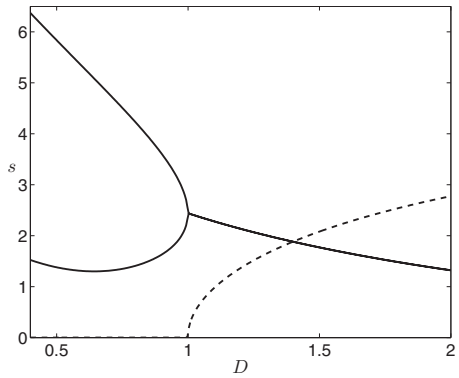

FIG. 9. Two largest eigenvalues when $V=4$, $k=4$, and $\mathrm{Pe}=10^4$. The solid line denotes the real part of the two most dominant eigenvalues and the dashed line the magnitude of the imaginary part. A transition to oscillating instability occurs as the system passes through $D=1$.

$D<1$. In Fig. 10 we show marginal stability curves for voltages $V=0.01,0.1,1,2,4$. We present the stability results using the control parameter identified in the low-current limit, namely, $L=\mathrm{Pe}\,\alpha^2(D-1)/(D+1)$. We find that the marginal stability curves depart from those in the low-current limit, but that the latter still provides a reasonable picture of the stability behavior. As the voltage increases, the critical value of L decreases.

The critical value of $L=-68$ at low current is reduced to $L=-30$ when $V=4$. Figure 10 allows for easy determination of the system's stability given the electrolyte properties Pe and D and the applied voltage. For example, when $V=4$ and $D=0.1$ the critical Péclet number for instability is approximately Pe=9.9. Since the critical Pe decreases with the decrease of D, in order to evaluate the minimal value of Pe for which bulk electroconvective instability occurs, we computed the critical Pe dependence on voltage for $D=0$. The resulting curve is presented in Fig. 11, suggesting $\mathrm{Pe}\approx 4.2$ as that minimal value.

When $D>1$, the MHM model predicted a critical voltage at which the system becomes unstable. For a finite Pe in the BE model, this threshold increases as the Péclet number is lowered toward more realistic values. In Fig. 12, we show the dependence of the marginally stable Péclet number versus voltage for different values of D and at some fixed wave number ($k=4$). The marginally stable values of voltage corresponding to the infinite-Péclet-number limit (MHM model) are shown by the dashed vertical lines. With increase of the voltage, the marginally stable Péclet number decreases, showing an ever-weakening dependence on D.

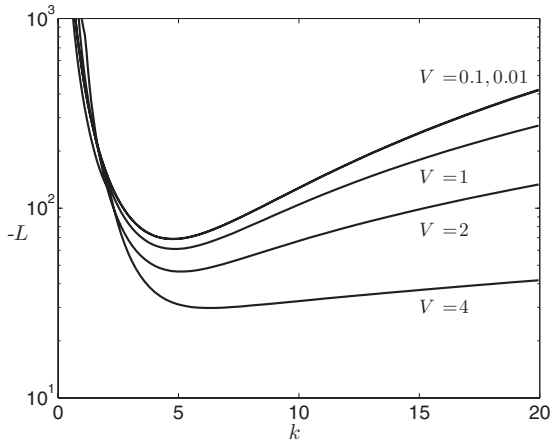

FIG. 10. Marginal stability curve at finite current, plotting the control parameter L vs wave number. The voltages are $V=0.01$, 0.1,1,2,4 and $D=0.1$.

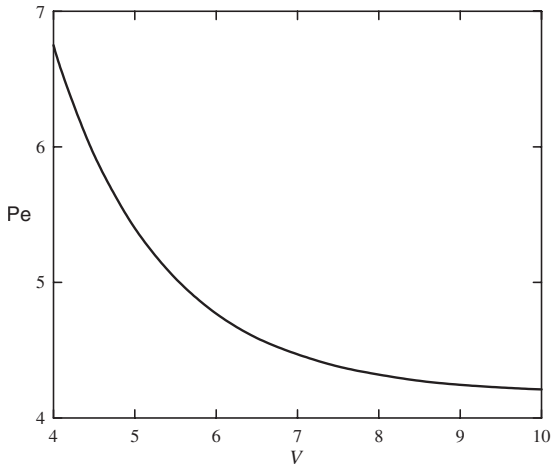

FIG. 11. Dependence of the critical value of Pe on voltage for $D=0$.

VII. CONCLUDING REMARKS

In this paper, we study the relation between the Hoburg and Melcher model of electroconvection in doped liquid dielectrics [37–40] and the bulk electroconvection model of the flow of an electrolyte due to the body forces exerted by an electric field acting upon the residual space charge of a locally quasielectroneutral ionic solution [20]. Considering both cases of low and high current we have traced the man-

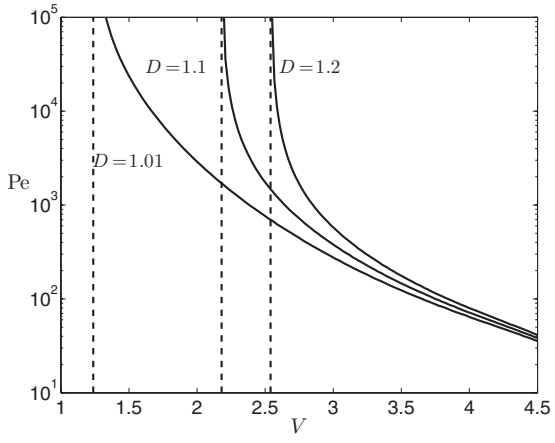

FIG. 12. Marginally stable Péclet number versus voltage for different values of $D>1$ and $k=4$. The dashed lines show the voltage computed from the MHM model (infinite Pe). The solid curves are computed from the BE model.

ner in which the bulk electroconvection model transforms into the leaky dielectric model in the limit of infinitely large Péclet number.

We have also demonstrated that the existence of bulk electroconvection depends critically upon the ratio of the cationic to anionic diffusivity, D. When the Péclet number is infinite, the case with equal ionic diffusivities becomes a bifurcation point, separating stable ($D>1$) and unstable ($D<1$) regimes in the low-current limit. At higher currents and very large Péclet numbers, we find that the system is unstable for any value of D but switches from a monotonic instability to an oscillatory one as D passes through unity.

When the Péclet number is finite and the anions are much more diffusive than the cations, an unreported bulk electroconvective instability is possible at low current. This instability can occur when the electroconvection Péclet number is on the order of $\mathrm{Pe}\sim 10$. This bulk instability mechanism may have some practical relevance for high-molecular-weight electrolytes.

ACKNOWLEDGMENT

This work was sponsored in part by the National Science Foundation through Grant No. CTS-0521845 (B.D.S.).

APPENDIX: DERIVATION OF THE LINEAR STABILITY SPECTRAL PROBLEM

In this appendix we formulate the linear stability problems for the concentration polarization solution (17)–(24) in the HM, MHM, and BE models. For this, we assume an infinitesimal flow $\mathbf{v}'$ which creates small two-dimensional fluctuations c',p',φ' in the concentration, pressure, and electrostatic potential. Let us consider a perturbation of the conduction solution (25) and (26) of the form

$$\underline{M}=\underline{M}_0+\underline{M}_1. \tag{A1}$$

Here,

$$\underline{M}_0=\begin{pmatrix} c_0(x) \\ \varphi_0(x) \\ \mathbf{v}_0\equiv\mathbf{0} \\ p_0(x) \end{pmatrix}, \quad \underline{M}_1=\begin{pmatrix} c'(x,y) \\ \varphi'(x,y) \\ \mathbf{v}'(x,y) \\ p'(x,y) \end{pmatrix} e^{st}, \tag{A2}$$

whence $\mathbf{v}'=v_x\mathbf{i}+v_y\mathbf{j}$ is the velocity perturbation vector.

Substitution of $\underline{M}$ into the BE problem (17)–(24), followed by linearization, yields a spectral problem for $(c',\varphi',\underline{v}',p')$ and s with the equations

$$\Delta\mathbf{v}'-\boldsymbol{\nabla}p'+\Delta\varphi_0\,\boldsymbol{\nabla}\varphi'+\Delta\varphi'\,\boldsymbol{\nabla}\varphi_0=\mathrm{Re}\,s\mathbf{v}', \tag{A3}$$

$$\frac{1}{\mathrm{Pe}}\Delta c'=v_x'\frac{dc_0}{dx}+sc', \tag{A4}$$

$$\frac{D-1}{D+1}\Delta c'+\boldsymbol{\nabla}\cdot(c_0\,\boldsymbol{\nabla}\varphi'+c'\,\boldsymbol{\nabla}\varphi_0)=0, \tag{A5}$$

$$\boldsymbol{\nabla}\cdot\mathbf{v}'=0. \tag{A6}$$

Applying the operator rot rot to the linearized Navier-Stokes equation (A3) yields

$$\Delta^2v_x'-\mathrm{Re}\,s\Delta v_x'=-\frac{\partial\varphi_0}{\partial x}\frac{\partial^2\Delta\varphi'}{\partial y^2}+\frac{\partial^3\varphi_0}{\partial x^3}\frac{\partial^2\varphi'}{\partial y^2}. \tag{A7}$$

Thus, the linear stability formulation reads

$$\frac{1}{\mathrm{Pe}}\Delta c'=\frac{I}{2}v_x'+sc', \tag{A8}$$

$$\frac{D-1}{D+1}\Delta c'+\frac{I}{2}\varphi_x'+c_0\Delta\varphi'+\frac{\partial}{\partial x}\left(\frac{I}{2+I(x-1/2)}c'\right)=0, \tag{A9}$$

$$\Delta^2v_x'-\mathrm{Re}\,s\Delta v_x'=-\frac{I}{2+I(x-1/2)}\frac{\partial^2\Delta\varphi'}{\partial y^2}+2\left(\frac{I}{2+I(x-1/2)}\right)^3\frac{\partial^2\varphi'}{\partial y^2}, \tag{A10}$$

with the following boundary conditions resulting from (21)–(24):

$$\left.\frac{\partial c'}{\partial x}\right|_{x=0}=\left.\left(\frac{I/2}{1-I/4}c'+(1-I/4)\frac{\partial\varphi'}{\partial x}\right)\right|_{x=0}=v_x'|_{x=0}=\left.\frac{\partial v_x'}{\partial x}\right|_{x=0}=0, \quad x=0 \quad \text{(left membrane — anode)}, \tag{A11}$$

$$\left.\frac{\partial c'}{\partial x}\right|_{x=1}=\left.\left(\frac{I/2}{1+I/4}c'+(1+I/4)\frac{\partial\varphi'}{\partial x}\right)\right|_{x=1}=v_x'|_{x=1}=\left.\frac{\partial v_x'}{\partial x}\right|_{x=1}=0, \quad x=1 \quad \text{(right membrane — cathode)}. \tag{A12}$$

The basic question we address is whether the boundary value problem (A8)–(A12) possesses a nontrivial solution for some value of the control parameter I.

[1] I. Rubinstein, E. Staude, and O. Kedem, Desalination **69**, 101 (1988).
[2] S. S. Dukhin and N. A. Mishchuk, Kolloidn. Zh. **51**, 659 (1989) (in Russian).
[3] I. Rubinstein and B. Zaltzman, Phys. Rev. E **62**, 2238 (2000).
[4] V. Fleury, J.-N. Chazalviel, and M. Rosso, Phys. Rev. E **48**, 1279 (1993).
[5] V. Fleury, J. H. Kaufman, and D. B. Hilbert, Nature (London)

367, 435 (1994).
[6] C. Livermore and P. Z. Wong, Phys. Rev. Lett. **72**, 3847 (1994).
[7] M. Trau, D. A. Saville, and I. A. Aksay, Science **272**, 706 (1996).
[8] J. A. Manzanares, W. D. Murphy, S. Mafe, and H. Reiss, J. Phys. Chem. **97**, 8524 (1993).
[9] A. Ajdari, Phys. Rev. E **61**, R45 (2000).
[10] H. A. Stone, A. D. Stroock, and A. Ajdari, Annu. Rev. Fluid Mech. **36**, 381 (2004).
[11] M. Z. Bazant and T. M. Squires, Phys. Rev. Lett. **92**, 066101 (2004).
[12] A. Ramos, H. Morgan, N. G. Green, A. González, and A. Castellanos, J. Appl. Phys. **97**, 084906 (2005).
[13] D. J. Laser and J. G. Santiago, J. Micromech. Microeng. **14**, 35 (2004).
[14] H. Lin, B. D. Storey, M. H. Oddy, C. H. Chen, and J. G. Santiago, Phys. Fluids **16**, 1922 (2004).
[15] C. Chen, H. Lin, S. K. Lele, and J. G. Santiago, J. Fluid Mech. **524**, 263 (2005).
[16] J. D. Posner and J. G. Santiago, J. Fluid Mech. **555**, 1 (2006).
[17] E. I. Belova, G. Y. Lopatkova, N. D. Pismenskaya, V. V. Nikonenko, C. Larchet, and G. Pourcelly, J. Phys. Chem. B **110**, 13458 (2006).
[18] N. D. Pismenskaya, V. V. Nikonenko, E. I. Belova, G. Y. Lopatkova, P. Sistat, G. Pourcelly, and C. Larchet, Russ. J. Electrochem. **43**, 307 (2007).
[19] R. Bruisma and S. Alexander, J. Chem. Phys. **92**, 3074 (1990).
[20] I. Rubinstein, Phys. Fluids A **3**, 2301 (1991).
[21] A. P. Grigin, Elektrokhimiya **28**, 307 (1992) (in Russian).
[22] A. P. Grigin, Elektrokhimiya **21**, 52 (1995) (in Russian).
[23] R. S. Alexandrov, A. P. Grigin, and A. P. Davydov, Russ. J. Electrochem. **38**, 1216 (2002).
[24] I. Rubinstein, T. Zaltzman, and B. Zaltzman, Phys. Fluids **7**, 1467 (1995).
[25] T. Zaltzman, Phys. Fluids **8**, 936 (1996).
[26] E. K. Zholkovskij, M. A. Vorotynsev, and E. Staude, J. Colloid Interface Sci. **181**, 28 (1996).
[27] I. Rubinstein, B. Zaltzman, and O. Kedem, J. Membr. Sci. **125**, 17 (1997).
[28] J. C. Baygents and F. Baldessari, Phys. Fluids **10**, 301 (1998).
[29] M. E. Buchanan and D. A. Saville, in Proceedings of AIChE Annual Meeting 1999, Dallas, TX, 1999 (unpublished).
[30] I. Rubinstein and B. Zaltzman, Math. Models Meth. Appl. Sci. **11**, 263 (2001).
[31] I. Rubinstein, B. Zaltzman, J. Pretz, and C. Linder, Russ. J. Electrochem. **38**, 853 (2002).
[32] I. Rubinstein and B. Zaltzman, Phys. Rev. E **68**, 032501 (2003).
[33] I. Lerman, I. Rubinstein, and B. Zaltzman, Phys. Rev. E **71**, 011506 (2005).
[34] I. Rubinstein, B. Zaltzman, and I. Lerman, Phys. Rev. E **72**, 011505 (2005).
[35] T. Pundik, I. Rubinstein, and B. Zaltzman, Phys. Rev. E **72**, 061502 (2005).
[36] B. Zaltzman and I. Rubinstein, J. Fluid Mech. **579**, 173 (2007).
[37] J. F. Hoburg and J. R. Melcher, J. Fluid Mech. **73**, 333 (1976).
[38] J. F. Hoburg and J. R. Melcher, Phys. Fluids **20**, 903 (1977).
[39] J. F. Hoburg, J. Fluid Mech. **84**, 291 (1978).
[40] D. A. Saville, Annu. Rev. Fluid Mech. **29**, 27 (1997).
[41] Z. A. Daya, S. W. Morris, and J. R. de Bruyn, Phys. Rev. E **55**, 2682 (1997).